8° SESSION D'ETUDES BIENNALE DE PHYSIQUE NUCLEAIRE

AUSSOIS 4 - 8 Février 1985

Institut de Physique Nucléaire et IN2P3

Université Claude Bernard Lyon 1

43, Bd. du 11 Novembre 1918 · 69622 Villeurbanne · Cedex · Tél.: (7) 889-81-24 poste 37-22

Télex : IPN Lyon 380 273 F

(59

RELATIVISTIC HEAVY ION COLLISIONS AND THE NUCLEAR EQUATION OF STATE

J. CUGNON

Université de Liège, Institut de Physique B5,

Sart Tilman, 4000 Liège 1, Belgique.

RELATIVISTIC HEAVY ION COLLISIONS AND THE NUCLEAR EQUATION OF STATE

J. CUGNON
Université de Liège, Institut de Physique B5,
Sart Tilman, 4000 Liège 1, Belgique.

ABSTRACT : The general properties of the nucleus-nucleus collisions in the GeV/A range are reviewed. It is shown that, despite of the very transient nature of the process, some observable quantities are linked with the formation of a dense, very excited state of the matter. It is not, however, quite clear whether these quantities are relevant for the bulk properties of the matter. The questions of the pion multiplicity and the deuteron to proton ratio are analyzed. The equation of state is tentatively derived for some values of the thermodynamical variables.

1. INTRODUCTION

The admitted objective of the relativistic nucleus-nucleus collisions is to determine the properties of nuclear matter under extreme conditions of temperature and density. The simplest of these properties are carried by the phase diagram and the equation of state (EOS). Very little is known for sure about the phase diagram, although a lot of speculations have been made. Strong theoretical conjectures are in support of the possibility of a phase transition between nuclear matter (sometimes called the hadronic gas or fluid to account for excitations of mesonic degrees of freedom) and the quark-gluon plasma [1]). On the same status, we place the liquid-gas phase transition at low temperatures and densities [2]). Other features of the phase diagram are much more speculative. We will not discuss these phase transitions, which are under intensive study and we will concentrate on the equation of state of the hadronic fluid. The latter is very important for testing the field theoretical approaches of nuclear matter [3,4]) (and even the more conventional views), for the understanding of the presupernovae matter [5]), of the collapse of a supernovae [5]) and of the structure of neutron stars [6]). It is also important for the nature of the phase transition towards quark-gluon plasma at low temperature [7]).

For the nucleus-nucleus collision, a dynamical process, to be relevant to the study of the EOS, a purely static property, two conditions have to be met :

(1) there should exist at some time during the collision, a part of the system, or better the whole system itself, which can be considered as in thermal (and possibly) in chemical equilibrium ;

(2) one has to single out observables which have been determined by the occurrence of such a state and which have been conserved by the subsequent evolution of the system.

It has now become clearer and clearer that in the GeV/A range, the matter is first strongly compressed at the beginning of the collision and then expands in a rather short time, even for strong interaction standards.The detail of the scenario is however not unique and can change from theory to theory. Therefore, only uncertain answers can be provided to the above questions. The total pion multiplicity, the strange particle yields [8]), the cluster yield and global variables [9,10]) have been proposed as possible testing quantities. The first and the third ones have even been used to tentatively extract information about the EOS. We will present the recent developments in these directions.

In Section 2, we recall some basic thermodynamics. In Section 3, we briefly discuss the essential features of the collision process. In Sections 4 and 5, we analyze the pion yield and the cluster yield successively. For the latter, we investigate the connection with the entropy. Finally, Section 6 contains our conclusion.

2. THERMODYNAMICS

The EOS (in the general sense) embodies the simplest static properties of an extended system, and appears as the relationship between the internal energy density and two thermodynamical variables. In nuclear physics, one usually uses physical quantities per nucleon. One may thus consider the following relationship

$$U/A = f(\rho, T) \quad , \qquad (2.1)$$

or using the natural variables (S denotes the entropy)

$$U/A = g(\frac{S}{A} , \rho) \quad . \qquad (2.2)$$

The nuclear matter EOS refers to Eq. (2.1) for an extended system of equal number of protons and neutrons, for which the Coulomb interaction has been artificially switched off. One may generalize the relation for other variables as the neutron excess $x = \frac{(N-Z)}{A}$:

$$\frac{U}{A} = f(\rho, x, T) = g(\frac{S}{A}, \rho, x) \quad . \qquad (2.3)$$

The internal energy per baryon is often divided into a thermal part and a compression part

$$\frac{U}{A} = \frac{E_{th}}{A} (\rho, x, T) + \frac{E_C}{A} (\rho, x) \quad , \qquad (2.4)$$

with

$$\frac{E_{th}}{A} (\rho, x, T=0) = 0 \quad . \qquad (2.5)$$

Let us stress that the division (2.4), although quite appealing, has a very limited meaning, except at $T = 0$. The thermal and compression energies, if respectively identified to the heat quantity and the work necessary to reach a state (ρ,T), are not uniquely defined by the values of the parameters (ρ,T). It is an old thermodynamical fact that they depend upon the path used to go from (ρ_0,T_0) to (ρ,T). Equation (2.4) corresponds to a transformation following an isoentrope at $(\frac{S}{A} = T = 0)$ followed by an isochore (ρ = constant).

It is also misleading to consider E_{th} as the average kinetic energy and E_C as the interaction energy. Obviously, at $T = 0$, there is a lot of kinetic energy inside nuclear matter. At the best, E_{th} can be tentatively identified as the excess of kinetic energy when the temperature is raised from $T = 0$.

The quantity $E_C/A(\rho,x)$ is well-known for $\rho \lesssim \rho_0$, from theoretical investigations [11]). Experimentally, only the two following points are known :

$$\frac{E_C}{A}(0,0) = 0 \quad , \quad \frac{E_C}{A}(\rho_o,0) = B_o = -16 \text{ MeV} \quad , \quad \rho_o \simeq 0.17 \text{ fm}^{-3} \quad . \tag{2.6}$$

An other experimentally known quantity is the compression modulus [12].

$$K = 9\,\rho^2 \frac{\partial^2}{\partial\rho^2}(E_c/A)\bigg|_{\rho=\rho_o} = 210 \pm 30 \text{ MeV} \quad . \tag{2.7}$$

These two figures are often summarized in the simplest manner as either of the following two guesses for the functional E_C :

$$\frac{E_C}{A}(\rho,0) = \frac{K}{18\,\rho\rho_o}(\rho-\rho_o)^2 + B_o \tag{2.8a}$$

$$\frac{E_C}{A}(\rho,0) = \frac{K}{18\,\rho_o^2}(\rho-\rho_o)^2 + B_o \quad . \tag{2.8b}$$

Nothing very much is known about the function E_{th} either. In view of this ignorance, the latter is often considered to be close to the Fermi gas value. In this case, one may generalize the formulae by incorporating the possible creation of pions and formation of Δ-resonances, if the latter are considered as particles. One has then for each species $i = N,\pi,\Delta$, $(\hbar = c = k = 1)$:

$$E_{th,i} = \frac{g_i}{2\pi^2}\,T^4\,\{(\frac{m_i}{T})^2\sum_{\ell=1}^{\infty}\ell^{-2}\,[3\,K_2(\frac{\ell\,m_i}{T}) + \frac{\ell\,m_i}{T}\,K_1(\frac{\ell\,m_i}{T})]\,(-\delta)^{\ell-1}\exp(\frac{\ell\,\mu_i}{T})\} \tag{2.9}$$

$$\rho_i = \frac{g_i}{2\pi^2}\,T^3\,\{(\frac{m_i}{T})^2\sum_{\ell=1}^{\infty}\frac{1}{\ell}\,K_2(\frac{\ell\,m_i}{T})(-\delta)^{\ell-1}\exp(\frac{\ell\,\mu_i}{T})\} \quad . \tag{2.10}$$

In these equations, g_i is the spin-isospin degeneracy, m_i is the particle mass and μ_i is the chemical potential for the species i. The quantity $\delta = -1$ for the bosons, +1 for the fermions. For Boltzmann particles, $\delta = 0$ and the summations reduce to the first term. The chemical potentials obey :

$$\mu_\pi = 0 \quad , \quad \mu_N = \mu_\Delta \quad . \tag{2.11}$$

For later purposes, we write explicitly the formulae obtained by using the non-relativistic Boltzmann approximation for the baryons and the relativistic Boltzmann approximation for the pions

$$E_{th} = \frac{4}{2\pi^2}\,N_N(m_N + \frac{3}{2}\,T) + \frac{16}{2\pi^2}\,N_\Delta(m_\Delta + \frac{3}{2}\,T) + \frac{3}{2\pi^2}\,N_\pi\,m_\pi^2\,T^2(3\,K_2(\frac{m_\pi}{T}) + \frac{m_\pi}{T}\,K_1(\frac{m_\pi}{T})) \tag{2.12}$$

$$\frac{N_\Delta}{N_N} = 4\,(\frac{m_\Delta}{m_N})^{3/2}\,e^{-\frac{m_\Delta - m_N}{T}} \quad , \tag{2.13}$$

and

$$N_\pi = \frac{3V}{2\pi^2}\,m_\pi^2\,T\,K_2(\frac{m_\pi}{T}) \simeq 3\,V(\frac{\pi}{2}\,m_\pi\,T)^{3/2}\,e^{-m_\pi/T} \quad . \tag{2.14}$$

In the last equation, V is the containing volume.

3. THE COLLISION PROCESS

The main features of the collision process between two heavy ions in the GeV/A range are more or less elucidated nowadays [13]), owing to the combined developments of the hydrodynamical theory and of the intranuclear cascade (INC) calculations, although the two approaches disagree with each other on many details. The process is characterized by the following points :

(1) there is a separation between the spectator nucleons, which experience very small momentum transfer and the participants, which are strongly interacting. The separation between the two types roughly follows the so-called clean-cut geometrical picture.

(2) The system of participants first undergoes a strong compression, at the end of which it is very much excited. Afterwards, it expands quite rapidly and desintegrates in many pieces : nucleons, pions, and light nuclei essentially. The spectra of these particles are more or less of the Boltzmann type (although not isotropic), which indicates that the available energy has been shared by many nucleons. This leads naturally to the following questions : (1) Has a dense equilibrated piece of matter been formed ? (2) Are there observables which have recorded the properties of this state ?

The answer to the first question is hard to be provided. Figure 1 shows

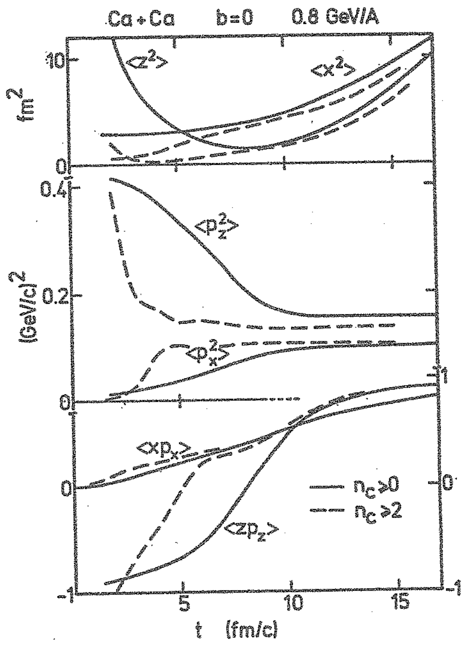

FIGURE 1.

Time evolution of various moments of the one-particle distribution function f_1. The non diagonal moments $\langle xp_x \rangle$ and $\langle zp_z \rangle$ have been normalized by dividing by $(\langle x^2 \rangle \langle p_x^2 \rangle)^{\frac{1}{2}}$ and $(\langle z^2 \rangle \langle p_z^2 \rangle)^{\frac{1}{2}}$, respectively. z stands along the beam axis. The full lines correspond to taking all the particles, whereas the dotted lines amount to selecting those that made two collisions at least. The figure refers to the c.m. frame. Adapted from Ref. 15.

the time evolution of several quantities, as calculated within the INC model of ref. [14]). They are various moments of the one-body distribution function $f_1(\vec{r},\vec{p},t)$, which gives the probability of finding at time t a baryon at position $\vec{r}$, with momentum $\vec{p}$. As can be seen, the system can hardly be considered as equilibrated at any time. One has to remind here that a necessary condition is the vanishing of $\vec{r}.\vec{p}$ correlations. At best, the system composed of the nucleons having made two collisions at least can be considered in equilibrium for a small time span around t = 8 fm/c after the beginning of the collisions. The relatively large mean free path of the nucleons is responsible for a non-equilibrated (non-relaxed in other words) component of nucleons having made no collision or one collision. This component is reduced in larger systems, which are thus more favourable to study dense matter.

As we said in the introduction, several observables have been proposed, in relation with the answer to the second question. Some of them are contained in Figures 2 and 3.

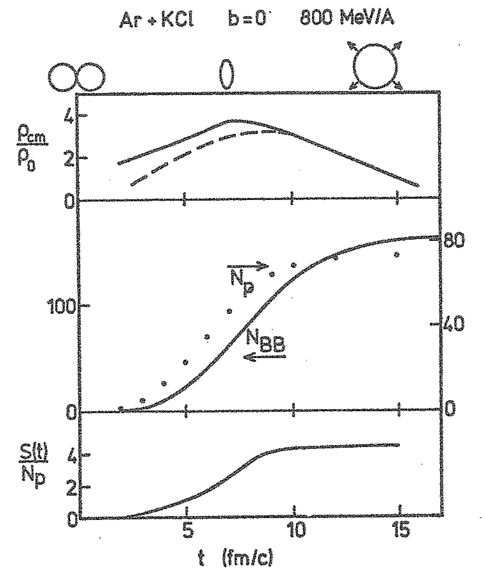

FIGURE 2.

Time evolution of the baryon density (dashed line : participants only, full line : all baryons included) normalized to the normal density of nuclear matter (top), of the number of baryon-baryon collisions (centre, scale on the left), of the number of participants (centre, scale on the right), and of the entropy of the participant system divided by the final number of participants (bottom). Taken from Ref. 15.

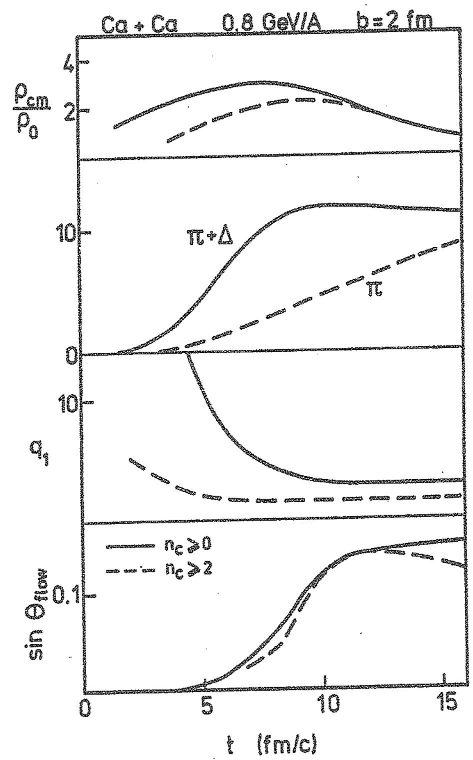

FIGURE 3.

Time evolution of several quantities for b = 2 fm Ca + Ca collisions at 800 MeV/A : baryon density at the c.m (top), pion and Δ abundances (second part), first aspect ratio (third part), flow angle (bottom). See text for detail. Same conventions as in Figure 2.

In Figure 2, it is shown that the entropy gained by the system is essentially fixed at the time of maximum compression. According to ref. [16]), the entropy is related to the deuteron and proton abundances (see Section 5).

Figure 3 displays other quantities of this kind. The possibility that the final pion abundance carries information about the dense state of the system has been first advanced in ref. [17]). This feature has been exploited by Stock's group[18]) as we explain in Section 4. The two lowest parts of Figure 3 are related to the second moments of the final momentum distribution (in the c.m. frame)

$$Q_{ij} = \int d^3p \; d^3r \; f_1(\vec{r},\vec{p}) \; p_i \; p_j \quad . \tag{3.1}$$

This tensor represents an ellipsoid which gives a rough idea of the momentum flow. The more elongated it is, the less isotropic the particle emission is. The orientation of the ellipsoid gives the preferred emission direction. The elongation is characterized by the so-called aspect ratio $q_1 = \lambda_1/\lambda_3$, the ratio between the largest and the smallest eigenvalues. The angle ϑ_{flow} between the largest axis of the ellipsoid and the beam axis is called the flow angle. These two quantities are manifestly determined before the end of the collision process, but they seem less correlated to the maximum density stage than the entropy and the total pion abundance.

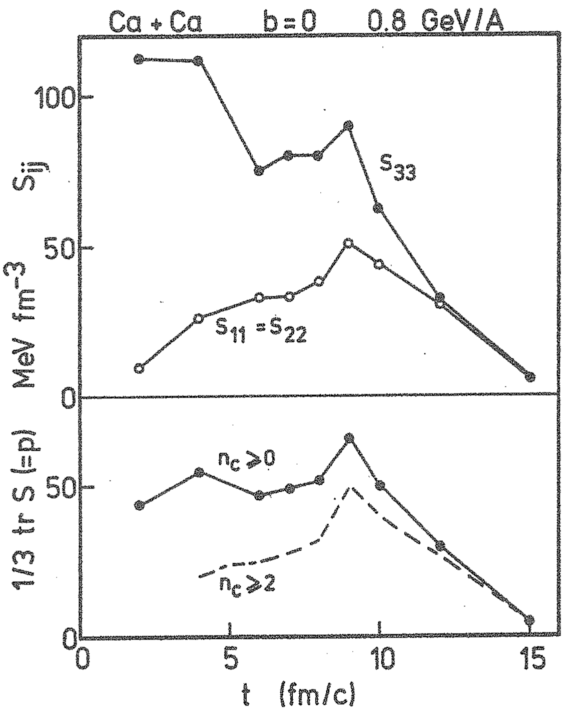

FIGURE 4.

INC calculation of the diagonal elements of the stress tensor near the c.m. of the system in central Ca + Ca collisions. The tensor is constructed by counting all the baryons in a test sphere of radius 1.1 fm in one hundred runs of the calculation. The second part of the figure gives the trace of the tensor divided by 3, when all the particles are taken into account (full line) or when only those that have made two collisions at least are retained (dashed line).

For the sake of completeness we have added in Figure 4 the time evolution of the pressure at the c.m., or more precisely of one third of the trace of the stress tensor. The upper part of the figure shows that indeed the stress tensor is not isotropic. The off-diagonal elements (not shown) are very small compared to the diagonal ones, which means that the viscosity plays no role in the vicinity of the c.m. The stress tensor for the $n_c \geq 2$ particles is almost isotropic everywhere, which gives the dotted curve in Figure 4 the physical meaning of a (partial) pressure.

4. THE PION MULTIPLICITY

One has first to understand (see Figure 3) why the total pion multiplicity keeps trace of the properties of the high density stage. This may be done on the basis of kinetic theory. First, one realizes that the Δ-production is very fast because of large cross-sections (≈ 20 mb) and isotropic production. If everything else remains constant, the Δ-abundance in an extended system evolves towards its equilibrium value as :

$$N_\Delta = N_\Delta^{eq}(1 - e^{-\tau/\tau_o}) \quad , \tag{4.1}$$

with

$$\tau_o \approx \frac{1}{2} \left(\frac{N_N}{N_\Delta}\right)_{eq} \rho_N \langle\sigma_{NN\to N\Delta}\, v\rangle \quad . \tag{4.2}$$

In the last equation, the brackets mean an average over the actual Δ and N momentum distributions, and v is the relative NN velocity. Typical values are $\rho_N \simeq 3\ \rho_o$, $(N_\Delta/N_N)_{eq} \simeq 0.2$ and $\tau = 2$ fm/c which is not larger than the duration of the high density state. Similarly the pions can be considered in chemical equilibrium with the other species, because of the large cross-section for the $\pi + N \to \Delta$ process. Therefore, it is a reasonable picture to consider the species in chemical equilibrium during the high density stage. However, it is not clear that thermal equilibrium is reached even in an acceptable approximation. Let us consider, for the time being, that it is the case. The question which naturally arises is : what keeps the chemical composition constant ? The answer lies in the properties of the expansion. The latter happens on a short time scale (≃ 3 fm/c), which tends to freeze the chemical composition. Moreover, the expansion is isoentropic, in all likelihood (see ref. [19]) and Figure 1). As a consequence, the Δ-population decreases, because of the lowering of the internal temperature (see Eq. (2.13)). On the contrary, the pion population increases because of the expanding volume. The net result is an almost constant π + Δ abundance during the expansion.

This observation has been exploited by R. Stock et al. [18]) to try to extract the EOS, more precisely, the function $E_C(\rho)$ (Eq. (2.6)). We present here their reasoning in a slightly modified presentation. With the same hypotheses as in Section 2, and assuming all the nucleons are participating, one can always divide the available energy E_o as

$$E_o = E_{th} + E_C + E_{flow} \quad . \tag{4.3}$$

The quantity E_{th} refers to the chaotic motion of the particles and E_{flow} refers to the overall flow motion of the hydrodynamical type. At the maximum compression time, $E_{flow} \simeq 0$. Equations (2.13-14) can be recast into

$$N_\pi + N_\Delta = f_{th}(E_{th},\rho_B) \quad , \tag{4.4}$$

where ρ_B is the baryon density. The function f_{th}, relevant for the thermal model cannot be put a simple analytical form, but can be constructed anyhow by eliminating T from the equations (2.12)-(2.14). One expects essentially a similar relationship in the INC model (as in other kinetic models). Therefore we write

$$N_\pi + N_\Delta = f_{INC}\ (E_{th},\rho_B) \quad , \tag{4.5}$$

where f_{INC} is different from f_{th} because of effects discussed below. In the INC model, and in thermal models as well, there is no compressional energy, and the first argument in (4.5) is essentially E_o, the available kinetic energy :

$$(N_\pi + N_\Delta)_{INC} = f_{INC}\ (E_o,\rho_B) \quad . \tag{4.6}$$

Now, if one accepts the INC model as a good model for transforming the available kinetic energy into pions, we may keep (4.5) and recast it into

$$N_{\pi}^{obs} = (N_{\pi} + N_{\Delta})_{exp} = f_{INC}(E_o - E_C(\rho_B), \rho_B) \quad . \qquad (4.7)$$

As expected, formula (4.6) overestimates the pion yield. Comparison between (4.7) and (4.6) may thus provide the function $E_C(\rho_B)$, if ρ_B is taken from the estimate of the INC model itself. The results are given in Figure 5.

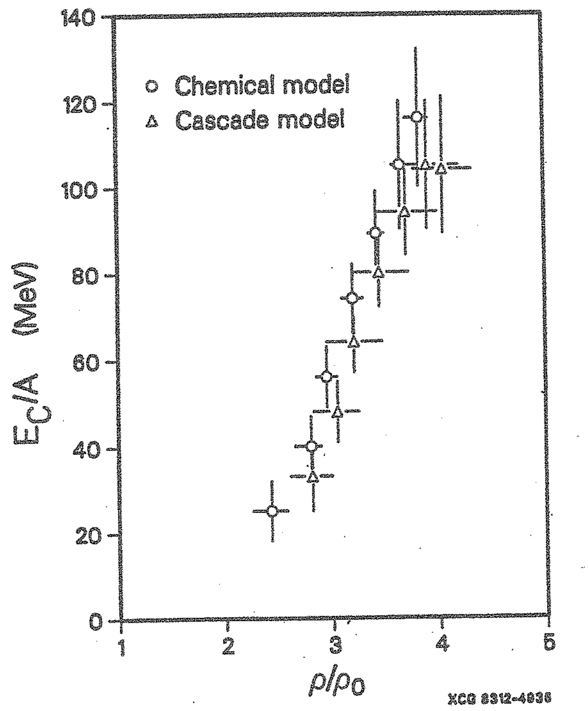

FIGURE 5.

Compression energy per nucleon as extracted from the comparison of the data with INC prediction (triangles) and with a chemical model calculation (dots). See text for detail. The investigated system is Ar + KCl. Adapted from Ref. 20.

The same argumentation can be carried out with the help of Eq. (4.4), with this time the thermal model expression, and the maximum density ρ_B evaluated through the Rankine-Hugoniot shock equation [20]). Once again, the pion multiplicity is overestimated and a compression energy must be introduced. With this procedure, one obtains a quantity E_C given by the open dots in Figure 5. It is gratifying to see that both approaches agree more or less. However, the first one is more reliable for the following reason : the function f_{INC} embodies, as in the real situation, off-equilibrium and finite size effects, which makes Eq. (2.12) only an idealisation. The main uncertainty, however, comes from the kinetic approach in general. It neglects the softening of the pion modes (or their modification, to say it in general) in dense matter.

5. THE ENTROPY

As it has been suggested, first by Siemens and Kapusta [16]), and also in refs. [19,21-22]), the entropy per nucleon can be related to the deuteron-like to proton-like ratio R_{dp} = "d"/"p" . We will assume below, in order to simplify the presentation, that the one-body proton and neutron distribution functions are proportional to the proton and neutron numbers, respectively :

$$\frac{A}{N} f_1^n = \frac{A}{Z} f_1^p = f_1 \quad . \tag{5.1}$$

The entropy per nucleon is then equal to

$$\frac{S}{A} = 1 - \langle \ell n\, f_1 \rangle + \ell n\, 2 - \frac{N}{A} \ell n \frac{N}{A} - \frac{Z}{A} \ell n \frac{Z}{A} \quad , \tag{5.2}$$

where the bracket means an average over the f_1-distribution itself

$$\langle \ell n\, f_1 \rangle = \frac{\int d^3r\, d^3p\, f_1(\vec{r},\vec{p})\, \ell n\, f_1(\vec{r},\vec{p})}{\int d^3r\, d^3p\, f_1(\vec{r},\vec{p})} \quad . \tag{5.3}$$

The number of deuteron-like structures in the final states is [19]

$$N_{"d"} = \frac{3}{4} \int d^3R\, d^3P \int d^3r\, d^3p\, f_2^{np}(\vec{R} + \frac{\vec{r}}{2}, \vec{R} - \frac{\vec{r}}{2}, \frac{\vec{P}}{2} + \vec{p}, \frac{\vec{P}}{2} - \vec{p})\, g_d(\vec{r},\vec{p}) \quad . \tag{5.4}$$

In this equation, f_2^{np} is the two-body distribution function for neutron-proton pairs in the final state and g_d is the Wigner representation of the deuteron density matrix. The factor 3/4 comes from the spins. The quantity $N_{"d"}$ gives the number of neutron-proton pairs which resemble a deuteron, irrespective of the rest of the system, no matter the pair is free from the rest, or embedded in a larger cluster. One refers to these pairs as deuteron-like objects. For clusters up to the α-particles, one has the following correspondence [19]

$$N_{"d"} = N_d + \frac{3}{2} (N_t + N_{^3He}) + 3\, N_{^4He} \quad . \tag{5.5}$$

Now, the quantity $N_{"d"}$ can be given a simple form, if the phase space extension of the system is much larger than the deuteron size, and if one makes the hypothesis of negligible correlations, $f_2^{np} \approx f_1^n f_1^p$. Then, Equation (5.4) becomes

$$R_{dp} = \frac{N_{"d"}}{N_{"p"}} = 6 \frac{N}{A} \langle f_1 \rangle \quad , \tag{5.6}$$

where $N_{"p"}$ is the proton-like (or charge) yield

$$N_{"p"} = \int d^3r\, d^3p\, f_1^p(\vec{r},\vec{p}) \quad . \tag{5.7}$$

Finite size effects can be evaluated analytically if both f_1 and g_d are taken as Gaussian functions :

$$f_1(\vec{r},\vec{p}) = \frac{A}{(\pi R_p \sqrt{2mT})^3} \exp\left[- \frac{r^2}{R_p} - \frac{p^2}{2mT}\right] \quad , \tag{5.8}$$

$$g_d(\vec{r},\vec{p}) = \frac{1}{(\pi r_o p_o)^3} \exp\left[- \frac{r^2}{r_o^2} - \frac{p^2}{p_o^2}\right] \quad . \tag{5.9}$$

In this case, one has

$$\frac{N_{"d"}}{N_{"p"}} = 6 \frac{N}{A} \langle f_1 \rangle\, X\left(\frac{r_o}{R_p}\right)\, Y\left(\frac{p_o}{\sqrt{mT}}\right) \tag{5.10}$$

with

$$X(x) = (1 + \frac{x^2}{2})^{-3/2} \quad , \tag{5.11}$$

$$Y(x) = (1 + x^2)^{-3/2} \quad . \tag{5.12}$$

In principle, an additional factor should be added to take care of a possible radial flow. The coefficients r_o and p_o are not independent ($r_o\, p_o \approx \hbar$), since the extension of g_d in phase space is equal to a natural unit cell. Now, in the case of a function f_1 as (5.7), there is a relation between $\langle \ell n\ f_1 \rangle$ and $\langle f_1 \rangle$:

$$\langle \ell n\ f_1 \rangle = -\ 3(1 - \ell n\ 2) + \ell n\ \langle f_1 \rangle \quad . \tag{5.13}$$

We draw the attention to the fact that the factor 3 replaces a factor 3/2 in the usual derivation, because, here, we have assumed a gaussian spatial distribution instead of a constant one. Gathering the results, we have the following generalization of the Siemens-Kapusta relation :

$$\frac{S}{A} = 4 + \ell n\ 3/2 + \frac{Z}{A}\ \ell n\ \frac{N}{Z} + \ell n\ X(\frac{r_o}{R_p})\ Y(\frac{p_o}{\sqrt{mT}}) - \ell n\ R_{dp} \quad . \tag{5.14}$$

This equation can be used to analyze the data. This calls for some preliminary remarks. First N, Z and A should refer to the participants which implies that deuterons in the so-called fragmentation region should be removed. This is done in the recent data and does not constitute a real problem. Second, since the equation (5.14) is a highly non-linear relation, one should apply it in narrow impact parameter intervals. This is the case for very recent data, which present the R_{dp} ratio as a function of the charge multiplicity (the quantity Z above), as shown in Figure 6.

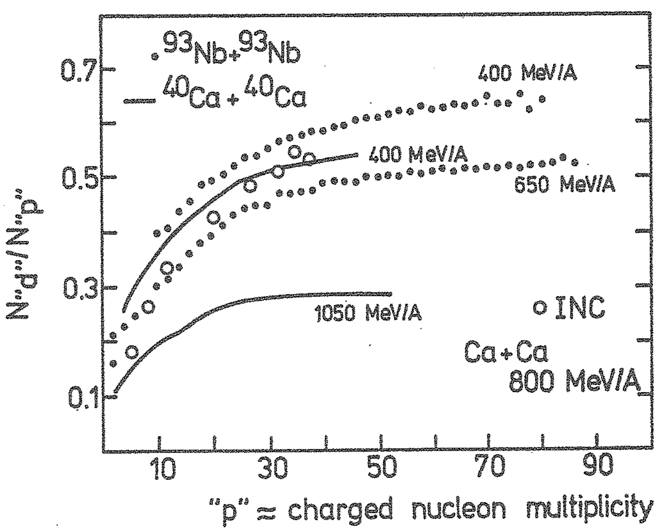

FIGURE 6.

Experimental "d"/"p" ratio versus charged multiplicity for four systems. The full dots are data from ref. [23]), the lines represent the data of ref. [24]) and the open dots are calculations from ref. [25]). For the latter the abscissa represents half the average participant number for several impact parameters ranging from zero to 7.15 fm.

A fit of the data can be attempted with the help of Eq. (5.10). But some assumptions have to be done in order to make the procedure meaningful. We closely follow here the lines of ref. [26]). First, the radius of the participants is assumed to be proportional to the third power of the participant number, for a given system. Hence, one may write (remember $Z = N_{"p"}$)

$$R_p = r_p Z^{1/3} = r_g(\frac{A}{Z})^{1/3} Z^{1/3} \quad . \tag{5.15}$$

Afterwards, for the sake of simplicity, $\langle f_1 \rangle$ is assumed to be constant, irrespective of the multiplicity. The relationship obtained in this way between the $N_{"d"}/N_{"p"}$ ratio and the multiplicity $N_{"p"}$ is tested in Figure 7, where the data of Figure 5 have been replotted after changes of scale, which make the relationship linear.

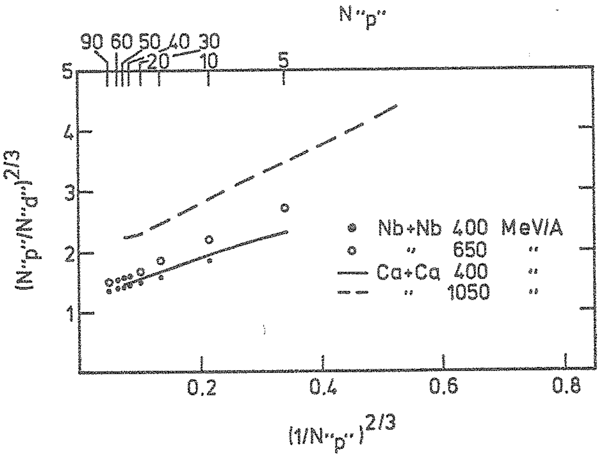

FIGURE 7.
Experimental data of Figure 6, presented in such a way to exhibit the relationship implied by Eqs. (5.10) and (5.15).
See text for detail.

The values extracted in this way are given in Table I. The ratio r_o/r_p comes directly from the fit. The other quantities are determined after r_o is properly chosen. We have taken r_o = 2 fm (indicated by the stars in Table I), a reasonable value. Then $\langle f_1 \rangle$ can be extracted, as well as the entropy through Eq. (5.10). In this analysis, $\langle f_1 \rangle$ and the entropy are independent of the multiplicity. All the variation of the $N_{"d"}/N_{"p"}$ is solely due to the factor X in Eq. (5.11) (Here, Y has been kept constant, since the observed momentum spectra are in general not very much dependent upon the multiplicity).

TABLE I.

System	Energy (GeV/A)	r_o/r_p	r_g * (fm)	$\langle f_1 \rangle$ *	$\frac{S}{A}$ *
Ca + Ca	0.4	2.34	0.67	0.29	4.53
Ca + Ca	1.05	2.31	0.69	0.17	5.07
Nb + Nb	0.4	2.23	0.68	0.29	4.53
Nb + Nb	0.65	2.65	0.57	0.27	4.60

Some uncertainty still remains in this analysis, although it is much more involved than the previous ones [16]). First, it is not sure that $\langle f_1 \rangle$ should be constant. There is a strong suspicion for a decrease of $\langle f_1 \rangle$ for low multiplicity [25,27]). Such a possibility would alter the extracted entropy for large (asymptotic) multiplicities.

By taking the asymptotic values, we get rid of the finite size (and possibly of off-equilibrium) effects, obtaining in this way the bulk or thermodynamic values of the entropy. We have still to find out the corresponding values for two other thermodynamic variables. Since we deal with limiting values, we can consider that the internal energy is the available energy, since for very large multiplicities the transparency will vanish. As for the density, one might think to determine it from two-proton correlation measurements. This is not correct, since the two-proton interferometry reveals the properties of the freeze-out at low density [28]), whereas the internal energy is equal to the available energy for the time of maximum density. One may try to determine the density by the fit of Figure 7 itself. Indeed, the parameter r_g in Table I can be translated in an average density by considering uniform distribution equivalent to the gaussian distribution (5.8) (in the sense of equal second moments). The results are contained in Table II.

TABLE II.

System	Energy (GeV/A)	$\frac{U}{A}$ (MeV)	$\frac{S}{A}$	$\frac{\rho}{\rho_o}$
Ca + Ca	0.4	95	4.53	2.13
Ca + Ca	1.05	233	5.07	2.07
Nb + Nb	0.4	95	4.53	2.13
Nb + Nb	0.65	150	4.60	3.60

However, this is not strictly correct, either, since the parameter r_g is relevant to the density at the formation of the deuterons. If one keeps the density as it is, the internal energy should be diminished from the flow energy gained by the system between the time of maximum density and the deuteron formation time. Even if the latter is about 30 %, this does not change very much the results as seen by Figure 8. An uncertainty on the energy introduces horizontal error bars.

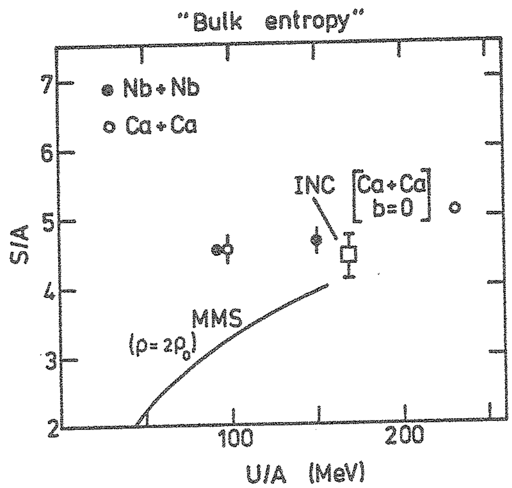

FIGURE 8.

Entropy as determined by the method of Section 5, from the data of Figure 6 (dots) and compared to the INC estimate of ref. [19]) and to the value corresponding to the EOS of ref. [29]).

The conclusion is that the bulk entropy is about 4.5 - 5 units, smaller by one unit than the previous estimate [16]). The INC estimate for central Ca + Ca collisions is close to the extracted values, but somewhat lower by about ~ 0.4 unit. Both are however larger than the predictions of a standard EOS, here the one of ref. [29]). It is too early to try to discuss the results of this investigation, but it now becomes clear that this method is very promising and opens the road to the determination of the bulk entropy for a wide domain.

6. CONCLUSION

We have shown that the nucleus-nucleus collision process, although a very transient process, generates for a short time a highly excited and compressed state, which can be considered as in thermal equilibrium in the limit of central collisions between large bodies. Moreover, some observables are fixed by this state and resist to further evolution during the expansion of the system. We have analyzed two of them, the total pion multiplicity and the entropy, which is related to the deuteron to proton ratio. Both of them carry information about the equation of state.

REFERENCES

1) G. Baym, in : "Quark Matter Conference 83", Brookhaven, September 1983.
2) B. Friedman and V.R. Pandharipande, Nucl. Phys. A361 (1981) 502.
3) J.D. Walecka, Ann. Phys. 83 (1974) 491.
4) T.D. Lee, G.C. Wick, in : "Mesons in Nuclei", eds M. Rho and D. Wilkinson, (North Holland Publishing Company, Amsterdam 1980) p. 867.
5) H.A. Bethe et al., Nucl. Phys. A324 (1979) 487.
6) M. Nauenberg and G. Chapline, Astr. J. 179 (1973) 277.
7) G. Chapline, GSI Meeting, October 1984.
8) S. Nagamiya, Phys. Rev. Lett. 49 (1982) 1383.
9) R. Stock, 5th High Energy Heavy Ion Study, Berkeley, 1981, LBL-12652.
10) R. Stocker, J.A. Maruhn and W. Greiner, Phys. Rev. Lett. 44 (1980) 725.
11) R.B. Wiringa, in : "Recent Progress in Many-Body Theories", Altenberg 1983, eds. H. Kümmel and M.L. Ristig (Springer-Verlag, Berlin 1984).
12) J.P. Blaizot, Phys. Rep. 64 (1980) 171.
13) S. Nagamiya and M. Gyulassy, Adv. Nucl. Phys. 13 (1984) 201.
14) J. Cugnon, D. Kinet and J. Vandermeulen, Nucl. Phys. A379 (1982) 553.
15) J. Cugnon and J. Vandermeulen, in : "Winter College on Nuclear Physics", Trieste, March 1984.
16) P.J. Siemens and J.I. Kapusta, Phys. Rev. Lett. 43 (1979) 1486.
17) J. Cugnon, T. Mizutani and J. Vandermeulen, Nucl. Phys. A352 (1981) 505.
18) R. Stock et al., Phys. Rev. Lett. 49 (1982) 1236.
19) G. Bertsch and J. Cugnon, Phys. Rev. C24 (1981) 2514.
20) J.W. Harris and R. Stock, preprint LBL-17054 (1984).
21) E.A. Remler, Phys. Rev. C25 (1982) 2974.
22) M. Gyulassy, K. Frankel and E.A. Remler, Nucl. Phys. A402 (1983) 596.
23) H.H. Gutbrod et al., Nucl. Phys. A397 (1982) 177c.
24) S. Nagamiya, in : "Proceedings of the International Conference on Nuclear Physics", P. Blasi and R.A. Ricci, eds. (Tipografia Compositori, Bologna, 1983) p. 431.
25) G. Bertsch and J. Cugnon, unpublished.
26) H.A. Gustafsson et al, GSI Meeting, October 1984.
27) J. Cugnon, GSI Meeting, October 1984.
28) H.A. Gustafsson et al., preprint LBL-17678 (1984).
29) I.N. Mishustin, F. Myrher and P.J. Siemens, Phys. Lett. 95B (1980) 361.